Research Article | Vol. 27, No. 10 | 13 May 2019 | OPTICS EXPRESS 14842
Optics EXPRESS

Optimization of acousto-optic optical frequency combs

NITHYANANDAN KANAGARAJ,[1] LEO DJEVARHIDJIAN,[1] VICENTE DURAN,[1,2] COME SCHNEBELIN,[1] AND HUGUES GUILLET DE CHATELLUS[1,*]

[1] *Univ. Grenoble Alpes, CNRS, LIPhy, 38000 Grenoble, France*
[2] *GROC-UJI, Institut of New Imaging Technologies, Universitat Jaume I, 12071 Castello, Spain*
[*] *hugues.guilletdechatellus@univ-grenoble-alpes.fr*

Abstract: Acousto-optic optical frequency combs can easily produce several hundreds of mutually coherent lines from a single laser, by successive frequency shifts in a loop containing an acousto-optic frequency shifter. They combine many advantages for multi-heterodyne interferometry and dual-comb spectroscopy. In this paper, we propose a model for an intuitive understanding of the performance of acousto-optic optical frequency combs in the steady state. Though relatively simple, the model qualitatively predicts the effect of various experimental parameters on the spectral characteristics of the comb and highlights the primordial role played by the saturation of the gain medium in the loop. The results are validated experimentally, offering a new insight in the performance and optimization of acousto-optic frequency combs.

1. Introduction

Optical frequency combs (OFCs) have led to numerous achievements in metrology, with dual-comb spectroscopy being one of the most paradigmatic applications [1–4]. Various sources of OFCs have been proposed over the years, including mode-locked lasers [5] and electro-optic OFCs [6]. Mode-locked lasers are capable of providing thousands of mutually coherent sharp lines. In these combs, the relative spacing between modes is set by the free spectral range (FSR) of the optical cavity, while the central frequency is fixed by the so-called carrier-to-envelope offset frequency. Because of the intrinsic drifts of the free-running cavity, both the FSR and the central frequency of the comb fluctuate over time. Efficient stabilization techniques have been proposed to control these two comb parameters, but they involve relatively complex and expensive locking systems [5]. Despite their high performance, a major disadvantage of mode-locked OFCs is the fact that the FSR is fixed by the length of the cavity, and it is not easily adjustable. To overcome these limitations, more flexible sources of OFCs have emerged over recent years. Electro-optic frequency combs are produced by phase and/or intensity modulation of a CW laser. The latter sets the central frequency of the comb and can be stabilized by means of an atomic or molecular transition, or a high-finesse cavity [7]. The comb FSR is equal to the frequency of the signal applied to the modulators. This system has obvious advantages over mode-locked OFCs, in terms of simplicity and tunability, but the bandwidth of the combs generated are limited to a few tens of lines [6]. As a consequence, methods such as the propagation in a highly non-linear fiber become indispensable to significantly extend the comb's bandwidth, but only at the cost of an increased complexity [7–9].

Of late, a different architecture has been proposed based on the successive shifts in frequency of a CW laser in a frequency shifting loop (FSL) [10–14]. The FSL typically contains a frequency shifter, an optical amplifier to compensate for the losses in the loop, and a tunable bandpass filter (TBPF). An input coupler enables to seed the loop with the CW laser, while an output coupler extracts a fraction of the field traveling in the FSL. The role of the TBPF is two-fold: (i) to control the number of lines, and (ii) to limit the spectral bandwidth of the amplified spontaneous

#360519 https://doi.org/10.1364/OE.27.014842
Journal © 2019 Received 21 Feb 2019; revised 19 Apr 2019; accepted 20 Apr 2019; published 8 May 2019

Optics EXPRESS

emission (ASE) inside the loop. Most of the approaches developed so far have made use of electro-optic (EO) modulators as frequency shifters (EOFS), so as to provide comb FSRs in the tens of GHz range, an option suitable for telecom applications [10]. However, due to the modest efficiency of single sideband EOFS and the detrimental role played by the ASE, the number of lines is generally limited only to a few tens [12].

Recently, we have demonstrated a particularly simple and robust FSL-based source of OFCs, involving an acousto-optic frequency shifter (AOFS) [15]. As compared to EOFSs, AOFSs are relatively simpler (no bias voltages are needed), and arguably efficient in terms of performance. Moreover, the extinction ratio of AOFSs exceeds 50 dB, whereas EOFSs produce an inevitable third harmonic, resulting in cross-talk effects in the generated comb lines [10], which is detrimental to OFC based applications. AOFSs typically induce a frequency shift in the tens to hundreds of MHz range, which can be positive or negative, depending on the acousto-optic interaction considered. Notice that placing in series two frequency shifters of opposite sign leads to arbitrarily small frequency shifts [16], thus making it possible to control the comb FSR over orders of magnitude, from DC to hundreds of MHz. We have shown that this so-called acousto-optic optical frequency comb (AO-OFCs) can contain more than 1000 mutually coherent lines, covering a bandwidth that exceeds 100 GHz, without the need for high-speed electronics [17, 18]. Recently, we have demonstrated the capability of this system for both self-heterodyne and dual-comb spectroscopy [16].

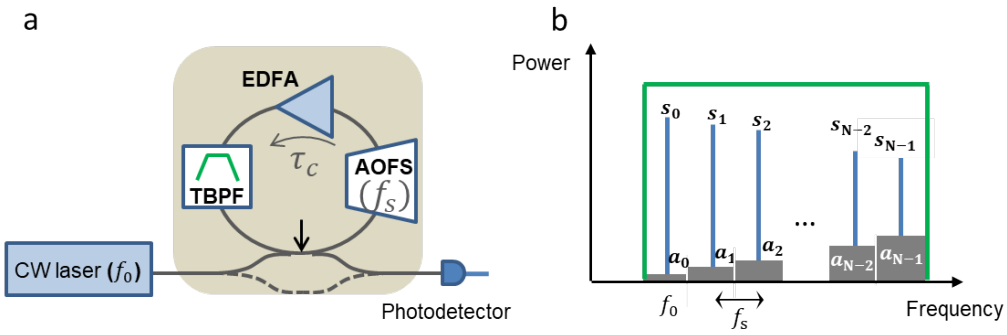

Fig. 1. (a) Sketch of an AO-FSL. The loop (travel time: τ_c) contains an amplifier (EDFA), an AOFS (driven at f_s), and a tunable bandpass filter (TBPF). Heterodyning the output of the FSL with the seed laser and performing a numerical Fourier transform enables one to record the AO-OFC. All power values considered in the model (s_n and a_n) are taken at the location of the arrow, i.e., between the input, and the output coupler. (b) Spectrum at the output of the FSL. The width of the flat-top TBPF (in green) is equal to Nf_s. The power of the line labelled by n is denoted by s_n. a_n is the ASE power in a frequency band of bandwidth f_s, centered around $f_n = f_0 + nf_s$.

In this paper, we propose an intuitive theoretical model to evaluate the functionality of AO-OFCs, and to optimize its performance depending on the system parameters. Our model is based on some simple yet valid hypotheses pertaining to AO-FSL as follows: (i) the system is considered to be in the steady state, (ii) the gain is the same for all the comb teeth, which is justified by the fact that the optical amplifiers considered here involve homogeneously broadened gain media, and (iii) the optical bandpass filter in the loop has an ideal flat-top transmission function (Fig. 1). With these assumptions, we can predict the typical exponential envelope of the AO-OFC, the power of the comb lines, and the spectral dependence of the ASE. The model proves the primary role of the gain saturation of the amplifier, and allows us to understand the

Optics EXPRESS

influence of numerous experimental parameters, such as the filter bandwidth, the comb FSR, the power of the injection laser, the transmission coefficient of the loop, the small signal gain of the amplifier and its noise figure. Following the theoretical understanding of the AO-OFCs, the second part of the manuscript is dedicated to the experimental validation of the model by recording the AO-OFC under various experimental conditions.

2. Theoretical model

As said, an AO-FSL includes an amplifier, an optical TBPF, and an AOFS driven at f_s (Fig. 1) [15–20]. The first coupler seeds the loop with a narrow-linewidth CW laser (< kHz), at the frequency f_0. We define s_0 as the power of the seed laser injected in the FSL. The second coupler enables to extract a fraction of the light traveling in the FSL. Owing to the successive frequency shifts in the loop, the output spectrum is a frequency comb, starting from f_0 and whose teeth are spaced by f_s. We define f_n as the frequency of the tooth number n, such that $f_n = f_0 + nf_s$. The total number of teeth, N, is in principle set by the bandwidth of the optical TBPF. Our model is based on the fact that in the steady-state, the power of the comb tooth n, denoted as s_n, is equal to the product of the power of tooth $n-1$ (s_{n-1}), and the *net* power transmission coefficient of the loop. We define this coefficient as $G \times T$, where G is the amplification factor introduced by the gain medium, and T is the power transmission coefficient of the loop excluding the amplifier. The recurrence relation $s_n = G \times T \times s_{n-1}$ leads to:

$$s_n = (G \times T)^n s_0. \tag{1}$$

It is obvious that the above expression manifests in an exponential variation of the comb envelope, which is an increasing (resp. decreasing) function when $G \times T > 1$ (resp. $G \times T < 1$). We now define a_n as the ASE power in a frequency band of width f_s, centered around f_n. Similarly, in the steady state, a_n is equal to the product of a_{n-1} by the power transmission coefficient of the round-trip loop, plus an additional term corresponding to the excess of ASE power emitted by the amplifier in a bandwidth of f_s. The latter is equal to: $a_0 = 2n_{sp}h\nu(G-1)f_s$, where n_{sp} is the spontaneous emission factor ($n_{\mathrm{sp}} > 1$), and h and ν (here, $\nu = f_n$) are respectively the Planck's constant and the central frequency of the photons [21, 22]. It is worth noting that n_{sp} can be related to the noise figure of the amplifier by: $NF = 10\log(2n_{\mathrm{sp}})$ [21]. Since the central frequency of the comb is orders of magnitude larger than its bandwidth, f_n can be approximated by f_0 for all values of n. Therefore, the resulting ASE power in the spectral band around f_n can be written as:

$$a_n = G \times T \times a_{n-1} + a_0, \tag{2}$$

where $a_0 = 2n_{\mathrm{sp}}hf_0(G-1)f_s$. Then:

$$a_n = \Sigma_{k=0}^{n}(GT)^k a_0 = \frac{1-(GT)^{n+1}}{1-GT}a_0. \tag{3}$$

Finally, the amplification factor is given by [22, 23]:

$$G = \exp\left(\frac{g_{ss}}{1+\frac{P_{\mathrm{tot}}}{P_{\mathrm{sat}}}}\right), \tag{4}$$

where g_{ss} is the (dimensionless) small signal gain and P_{sat} is the saturation power of the amplifier. We also define $G_{ss} = \exp(g_{ss})$ as the small signal amplification factor of the amplifier. The total power (P_{tot}) in the loop can be expressed as $P_{\mathrm{tot}} = P_{\mathrm{OFC}} + P_{\mathrm{ASE}}$, where $P_{\mathrm{OFC}} = \Sigma_{n=0}^{N-1}s_n$ and $P_{\mathrm{ASE}} = \Sigma_{n=0}^{N-1}a_n$. Finally, it is convenient to define the figure of merit of the AO-OFC as: $\mathrm{FoM} = P_{\mathrm{OFC}}/P_{\mathrm{ASE}}$.

Optics EXPRESS

Equations (1)–(4) are sufficient to determine the spectrum at the output of an injected AO-FSL, that is, the power of the comb teeth and of the ASE. To provide a comprehensive picture of the characteristics of the AO-OFCS, in what follows, we briefly investigate the influence of various experimental parameters, such as the width of the TBPF (*i.e.* the number of teeth, N), the comb FSR (f_s), the seed power (s_0), the noise figure (NF), the small signal amplification factor of the amplifier (G_{ss}), and the transmission coefficient of the loop (T). To highlight the effect of the individual parameters on the output spectrum, without any loss of generality, we keep the rest of the system parameters constant. We choose to represent the power of comb teeth (s_n, solid lines) and the ASE (a_n, dashed lines) as a function of the frequency bin labeled by n [Figs. 2–4]. For all plots, we also compute the corresponding FoM.

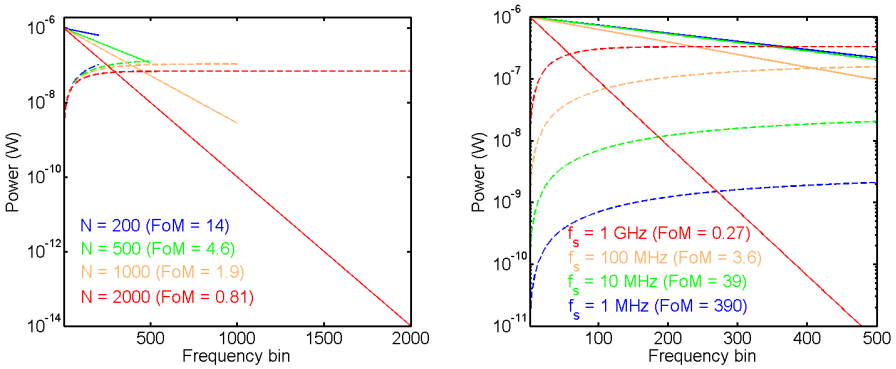

(a) (b)

Fig. 2. Influence of (a) the filter bandwidth (number of comb lines) and (b) the FSR on the comb (solid lines) and on the ASE spectrum (dashed lines). Unless specified in the plots, the default parameters have the following values: $\lambda_0 = c/f_0 = 1.55$ μm (wavelength of the seed laser), $N = 500$, $s_0 = 1$ μW, $G_{ss} = 100$, $P_{sat} = 300$ μW, $T = 0.1$, $f_s = 80$ MHz, and $NF = 5.5$ dB.

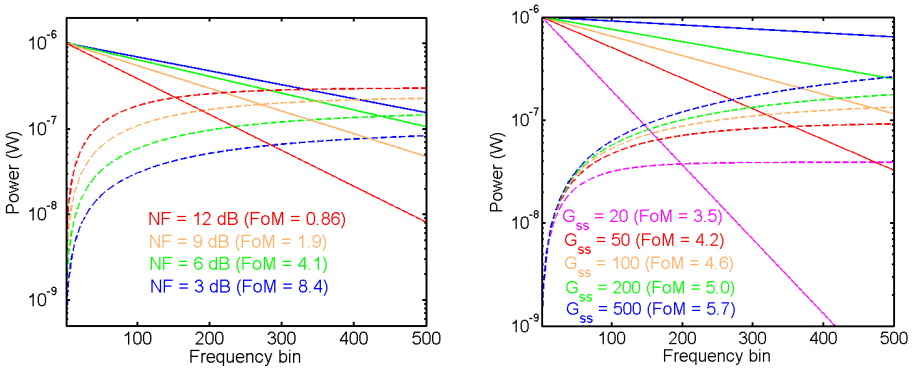

(a) (b)

Fig. 3. Role of characteristic parameters of the amplifier on the comb and ASE: (a) noise figure of the amplifier, and (b) small signal amplification factor.

It is apparent from Fig. 2 that the plots corresponding to the comb lines are linear in logarithmic scale; this behaviour is attributed to the exponential variation of the comb envelope, evidenced

Optics EXPRESS

by Eq. (1). Depending on the control parameters set by the experimental conditions, the shape of the ASE spectrum changes from a logarithmic function to an approximately constant value. The effect of the filter bandwidth on the output spectrum is shown in Fig. 2(a). In this plot, it can be seen that any increase in the filter bandwidth provides more spectral lines, but this leads to a higher negative slope of the comb, as a result of the saturation of the amplifier gain. Another tunable parameter in the loop is the FSR, which in AO-OFCs is set by the frequency of the signal driving the AOFS. We show in Fig. 2(b) the slope of the frequency comb and the ASE power for different values of the FSR. Note that the ASE grows significantly when the FSR is increased, which has a detrimental effect on the comb, accentuating the negative slope of the spectrum, due to the effect of gain saturation.

We show in Fig. 3 the characteristics of two important amplification parameters of AO-OFCs, namely, the noise figure of the amplifier, and the small signal gain. As expected, increasing the noise figure of the amplifier makes the power of ASE grow inside the loop. The saturation of the gain thus entails a reduction in the power of the comb [Fig. 3(a)]. Concerning the small signal gain, its influence is straightforward, since a higher value of G_{ss} produces a monotonous increase of both the power of the frequency comb and the ASE, as shown in the Fig. 3(b).

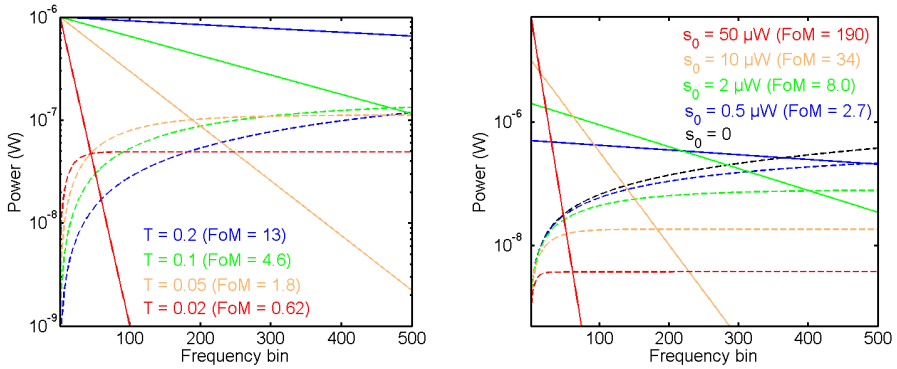

Fig. 4. Influence of (a) the transmission coefficient of the FSL and (b) the injection power on the comb and ASE spectrum.

In Fig. 4(a), we show the effect of the transmission coefficient T, which is in a way equivalent to vary the losses of the loop. As can be observed, the decrease of T leads to a high negative slope (and then to a reduced bandwidth), owing to the fact that the saturation of the gain does not make it possible to compensate for the increase in the loop losses. As one of the important control parameters of the system, we study the effect of the seed power in the output spectrum for some representative values of s_0, as is depicted in Fig. 4(b). As expected, the increase of s_0 reduces the number of comb lines due to the strong gain saturation at high seed powers.
For additional insight, the slope of the comb envelope is calculated as:

$$\text{slope} = 10\log(s_{n+1}/s_n), \tag{5}$$

where the comb power is deduced from Eqs. (1)–(4). Figure 5 represents this slope as function of the two parameters T and s_0. As expected, the comb envelope becomes flatter as the transmission coefficient of the loop is increased, and also when the injection power is decreased.

Finally, a particularly interesting case for practical applications, is the ideal situation where all comb teeth have the same power (flat-top OFC). Then $G = 1/T$, and the expressions of s_n and

Optics EXPRESS

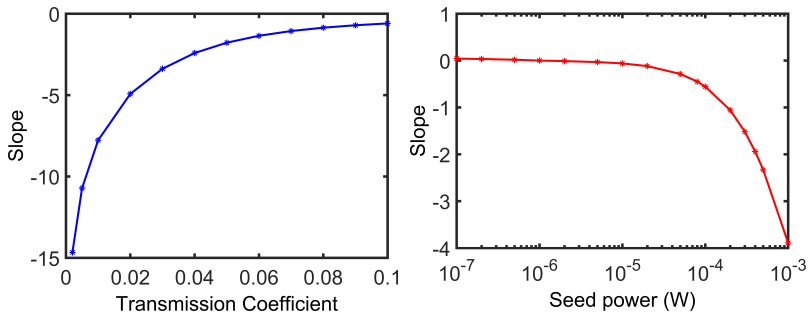

(a) (b)

Fig. 5. (a) Variation of the comb slope with the transmission coefficient (T) for the following parameters: $N = 500$, $s_0 = 1$ μw, $G_{ss} = 20$, $P_{sat} = 30$ μW, $f_s = 80$ MHz, and $NF = 5.5$ dB. (b) Variation of the comb slope with the seed power s_0 ($N = 500$, $G_{ss} = 100$, $P_{sat} = 700$ μW, $T = 0.1$, $f_s = 80$ MHz, and $NF = 5.5$ dB).

a_n are particularly simple: $s_n = s_0$, and $a_n = (n+1)a_0$. The total comb and ASE powers write respectively: $P_{\mathrm{OFC}} = Ns_0$ and $P_{\mathrm{ASE}} = N(N+1)a_0/2$. Finally, the FoM writes:

$$\mathrm{FoM} = \frac{s_0}{(N+1)n_{sp}hf_0(1/T-1)f_s} \simeq \frac{Ts_0}{n_{sp}hf_0Nf_s}. \tag{6}$$

This relationship highlights the parameters that play a critical role in the FoM. Interestingly, the AO-OFC FoM scales as the inverse of the total bandwidth (Nf_s), which provides an intrinsic limitation to the generation of broadband AO-OFCs. On the other hand, increasing T (*i.e.* minimizing the losses of the FSL), and increasing the seed power both enhance the FoM.

3. Experimental results

In order to validate the model, we performed a number of experiments on a fiber-based FSL. We particularly restricted ourselves to the influence of two readily controllable parameters in our setup, namely, the injection power and the losses of the loop. The setup we developed consists of a polarization-maintained fiber-optic loop, injected with a narrow linewidth CW laser (<kHz) at 1550 nm. The seed power is adjusted via a variable optical attenuator and measured using a power meter. As described earlier, the loop includes a TBPF and an Erbium-doped fiber amplifier (EDFA), see Fig. 1. The FSL travel time (τ_c) is ≈ 110 ns, a value that is set by the length of the fiber loop. In the present configuration of FSL, we employ two AOFSs that introduce frequency shifts with opposite signs, so as to produce a net (positive) shift equal to 50 kHz. The choice of this value is determined by the bandwidth of our detection system: since the optical comb is measured by heterodyning with a fraction of the injection laser, the bandwidths of the AO-OFC and of the RF signal produced by the photodetector are equal (no bandwidth compression) [16]. As a consequence, the spectral bandwidth of the comb must be less than the detection bandwidth (100 MHz in our case). In order to reduce the effect of intra-mode beat notes (produced by the interference of comb modes themselves), the power of the reference arm (dashed line in Fig. 1) is much higher that the average power emerging from the FSL. Since the comb FSR is much smaller than the frequency resolution of the TBPF (a few GHz), one cannot consider here the filter transfer function as a perfect flat-top with steep edges, but rather as a super-Gaussian profile, with a minimum bandwidth of a few GHz. However we adjusted the filter window, so that its central frequency corresponds to f_0. Since the total bandwidth of the comb does not exceed 100 MHz, therefore, we can consider that all comb lines encounter the same transmission coefficient.

Optics EXPRESS

It is worth mentioning that, although the self-heterodyne technique is widely adapted to measure the comb lines, in most cases our technique fails to provide an accurate measurement of the ASE spectrum. This is due to the limited dynamic range of our detection chain. The latter is based on a 12 bits digital oscilloscope, which sets a limitation on the smallest detectable optical power. More precisely, the power ratio between the reference laser and the ASE (a_0) is typically 100 dB, much larger than the dynamic range of the detection chain (72 dB). Therefore, we limit our experimental measurements to the characterization of the comb lines.

In a first set of experiments, illustrated in Fig. 6, we show the exponentially decreasing shape of the spectrum predicted by our theoretical model. The insets on display in Fig. 6 are for visual clarity to appreciate combs individual characteristics at different frequency range. In Fig. 7 we also plot the slope of the comb under different experimental conditions by maneuvering the amplification factor G and the transmission coefficient T.

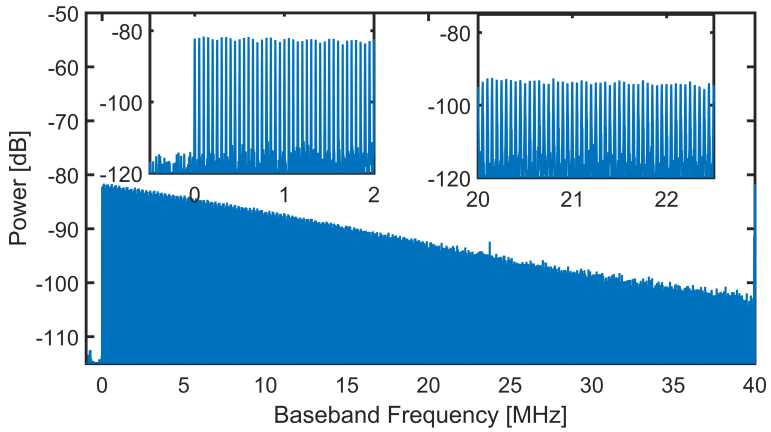

Fig. 6. Representative example of heterodyne measurement of an AO-OFC for f_s = 50 kHz. More than 800 lines are generated in the FSL. The ripples in the left inset are due to numerical artefacts of the digital sampling oscilloscope.

To do this, we measure the transmission coefficients across all components of the loop excluding the EDFA, such as couplers, connectors, TBPF, AOFS and fibers. The transmission coefficient T is the product of the transmission coefficients of all the components of the loop. Particularly, we can reliably control T by varying the amplitude of the signal applied to the AOFSs, as it directly affects the diffraction efficiency of the shifter and thus accounts for the AOFS loss. The amplification factor G of the gain medium is measured by inserting two 10 dB couplers before and after the EDFA, and measuring the input and output powers. We evaluate the slope of the spectrum for about 60 sets of parameters, by varying the pump current of the EDFA (i.e., the value of G), the transmission coefficient T, and the power of the seed laser s_0. The computed slope critically depends on the product $G \times T$ of the loop as shown in Fig. 7. It is observed that as long as the product $G \times T$ is less than 1, the experimental points follow the theoretical curve (in red) based on Eq. (1), which is a clear manifestation that the proposed model satisfactorily agrees with the experimental measurements. On the other hand, when the quantity $G \times T$ is greater than unity (which can be obtained at high pump current of the EDFA), the spectra obtained experimentally are very unstable, and the comb slope remains negative. This apparent contradiction is likely to come from the fact that the experimental determination of the gain by the method described above is overestimated here, since in this case, the EDFA generates a high level of ASE.

Optics EXPRESS

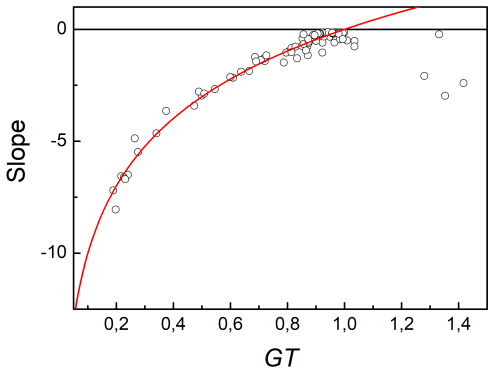

Fig. 7. Slope of the comb envelope measured in different experimental conditions, as a function of the product $G \times T$. The red curve is the function: slope $= 10 \log(G \times T)$.

For a comprehensive picture and to facilitate comparison with the theoretical prediction illustrated in Fig. 4, we show the influence of T and s_0. It is clear from Fig. 4 and Fig. 8 that the global trend of OFCs obtained from both theory and experiment agrees fairly well. Additional insight can be inferred by comparing the theoretically computed slope [Fig. 5] with the slope obtained from the experimental recordings shown in Fig. 9. Again, a qualitative agreement is apparent between theory and experiment.

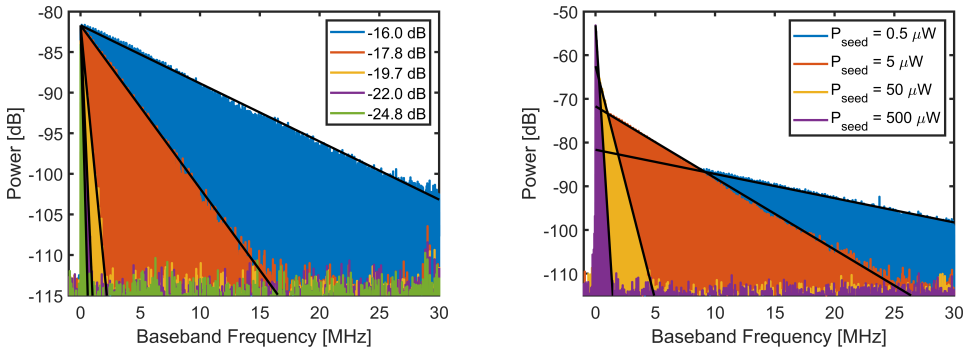

Fig. 8. (a) Influence of the transmission coefficient of the FSL (T, in dB) on the AO-OFC. (b) Influence of injection power.

4. Discussion and conclusions

We have proposed a simple yet efficient theoretical model for an intuitive understanding of the performance and optimization of acousto-optic frequency combs in the steady-state. The model is based on several valid hypotheses pertaining to an all-fiber FSL. By taking into account the effect of saturation of the gain and the amplified spontaneous emission, our model has demonstrated to predict the shape of the comb. The expressions to describe the envelope of the comb spectrum (as well as the ASE power) have been deduced from a recurrence relation between the teeth of the OFCs. We have found that the shape of the comb is described by a decreasing exponential function, which corresponds to a straight line with negative slope in the logarithmic scale. This

Optics EXPRESS

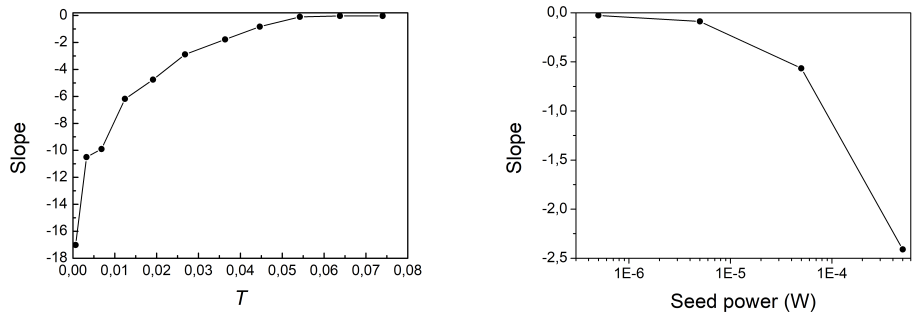

Fig. 9. Experimental variation of the comb slope with (a) the transmission coefficient, and (b) the seed power.

exponential envelope is directly related to the product of the EDFA amplification factor, G, and the transmission coefficient of the FSL excluding the EDFA, T. We studied the influence of several parameters, such as the comb FSR, the number of lines (or, equivalently, the bandwidth of the optical filter), the transmission coefficient of the loop, the power of the injection laser, the small gain signal, and the noise figure of the amplifier. These results help us to define the key parameters, that enable to optimize the AO-OFC. In all cases, using amplifiers with small noise factor and reducing the losses of the loop (*i.e.* increasing the transmission of the loop) have a positive influence on both the comb flatness and the FoM. The saturation power of the amplifier is also an important parameter. Producing broadband combs with constant line power would require maintaining the gain level to $G = 1/T$ over a large bandwidth. This can be achieved by means of amplifiers with a large saturation power. However, the seed power has a more subtle influence. For instance, increasing the injection power tends to increase the FoM, but to decrease the comb slope. Therefore, the parameters should be defined according to the target. Once the above key points are taken into account in the loop design, one can produce a broad comb with a large number of lines and a very small power decrease along the entire optical spectrum (see, for instance [17]). We have proven that our model can support a number of experimental observations under different settings. Thus, we have experimentally verified that the shape of the comb is effectively exponential decreasing, and that the slope is related to the net transmission coefficient of the loop, $G \times T$. We have also shown the influence of the injection power on the saturation of the amplifier and on the comb shape. It is worth noting that the present theoretical model considers the filter with a flat-top transmission function. To account for more realistic experimental conditions, one can easily modify Eqs. (1) and (3) by considering the spectral dependence of the filter's transmission.

To conclude, an AO-OFC is an easily implementable and emerging technique for the generation of high quality broadband OFCs, which can find applications, beyond spectroscopy, in many cutting-edge areas of technology, such as distance ranging and fiber sensing [24–27]. Despite its relative simplicity, the present model is a valuable tool to optimize the comb performance, depending on the targeted application. Besides, it is a step-forward towards the comprehensive understanding of AO-FSLs. A more complete model to describe the propagation of light inside the loop, taking into account the dynamics of the gain medium using laser rate equations, will be published elsewhere.

Optics EXPRESS

Funding

Agence Nationale de la Recherche (ANR) (ANR 14-CE32-0022, ANR-16-ASTR-015), Direction Générale de l'Armement (DGA ANR-16-ASTR-015), Université Grenoble-Alpes (AAP AGIR, pôle PEM, 2016), Ministerio de Ciencia, Innovación y Universidades (RYC-2017-23668).

Acknowledgments

We acknowledge Vincent Billault and Vincent Crozatier (Thales Research and Technology) for useful discussions.

References

1. T. Udem, R. Holzwarth, and T. W. Hänsch, "Optical frequency metrology," Nature **416**, 232–237 (2002).
2. I. Coddington, N. Newbury, and W. Swann, "Dual-comb spectroscopy," Optica **3**, 414–426 (2016).
3. D. A. Long, A. J. Fleisher, K. O. Douglass, S. E. Maxwell, K. Bielsk, J. T. Hodges, and D. F. Plusquellic, "Multiheterodyne spectroscopy with optical frequency combs generated from a continuous-wave laser," Opt. Lett. **39**, 2688–2690 (2014).
4. V. Durán, S. Tainta, and V. Torres-Company, "Ultrafast electro-optic dual-comb interferometry," Opt. Express **23**, 30557–30569 (2015).
5. I. Coddington, W. C. Swann, and N. R. Newbury, "Coherent multiheterodyne spectroscopy using stabilized optical frequency combs," Phys. Rev. Lett. **100**, 013902 (2008).
6. V. Torres-Company and A. M. Weiner, "Optical frequency comb technology for ultra-broadband radio-frequency photonics," Laser Photonics Rev. **8**, 368–393 (2014).
7. K. Beha, D. C. Cole, P. Del Haye, A. Coillet, S. A. Diddams, and S. B. Papp, "Electronic synthesis of light," Optica **4**, 406–411 (2017).
8. G. Millot, S. Pitois, M. Yan, T. Hovannysyan, A. Bendahmane, T. W. Hänsch, and N. Picqué, "Frequency-agile dual-comb spectroscopy," Nat. Photonics **10**, 27–30 (2016).
9. V. Duran, P. A. Andrekson, and V. Torres-Company, "Electro-optic dual-comb interferometry over 40 nm bandwidth," Opt. Lett. **41**, 4190–4193 (2016).
10. J. Li, X. Li, X. Zhang, F. Tian, and L. Xi, "Analysis of the stability and optimizing operation of the single-side-band modulator based on recirculating frequency shifter used for the T-bit/s optical communication transmission," Opt. Express **18**, 17597–17609 (2010).
11. F. Tian, X. Zhang, J. Li, and L. Xi, "Generation of 50 stable frequency-locked optical carriers for tb/s multicarrier optical transmission using a recirculating frequency shifter," J. Light. Technol. **29**, 1085–1091 (2011).
12. H. Tu, L. Xi, X. Zhang, X. Zhang, J. Lin, and W. Meng, "Analysis of the performance of optical frequency comb based on recirculating frequency shifter influenced by an Er-doped fiber amplifier," Photon. Res. **1**, 88–91 (2013).
13. J. Li, X. Zhang, Z. Li, X. Zhang, G. Li, and C. Lu, "Theoretical studies on the polarizationmodulator-based single-side-band modulator used for generation of optical multicarrier," Opt. Express **22**, 14087–14095 (2014).
14. J. Lin, L. Xi, J. Li, X. Zhang, X. Zhang, and S. Ahmad Niazi, "Low noise optical multi-carrier generation using optical-FIR filter for ASE noise suppression in re-circulating frequency shifter loop," Opt. Express **22**, 7852–7864 (2014).
15. H. Guillet de Chatellus, O. Jacquin, O. Hugon, W. Glastre, E. Lacot, J. Marklof, "Generation of ultrahigh and tunable repetition rates in CW injection-seeded frequency-shifted feedback lasers," Opt. Express **21**, 15065–15074 (2013).
16. V. Durán, C. Schnébelin, and H. Guillet de Chatellus, "Coherent multi-heterodyne spectroscopy using acousto-optic frequency combs," Opt. Express **26**, 13800–13809 (2018).
17. H. Guillet de Chatellus, L. Romero Cortés, and J. Azaña, "Arbitrary energy-preserving control of the free spectral range of an optical frequency comb over six orders of magnitude through self-imaging," Opt. Express **26**, 21069–21085 (2018).
18. H. Guillet de Chatellus, L. Romero Cortés, C. Schnébelin, M. Burla, and J. Azaña, "Reconfigurable photonic generation of broadband chirped waveforms using a single CW laser and low-frequency electronics," Nat. Commun. **9**, 2438 (2018).
19. H. Guillet de Chatellus, E. Lacot, W. Glastre, O. Jacquin, O. Hugon, "Theory of Talbot lasers," Phys. Rev. A **88**, 033828 (2013).
20. H. Guillet de Chatellus, L. Romero Cortés and J. Azaña, "Optical real-time Fourier transformation with kHz resolutions," Optica **3**, 1–5 (2016).
21. G. Kweon, "Noise figure of optical amplifiers," J. Korean Phys. Soc. **41**, 617–628 (2002).
22. G. Agrawal, *Applications of Nonlinear Fiber Optics* (Academic, Inc., 2008).
23. R. Paschotta, article on "gain saturation" in the *Encyclopedia of Laser Physics and Technology*, 1st ed. (Wiley-VCH, 2008).
24. I. Coddington, W. C. Swann, L. Nenadovic, and N. R. Newbury, "Rapid and precise absolute distance measurements at long range," Nature Photon. **3**, 351–356 (2009).

Optics EXPRESS

25. E. L Teleanu, V. Durán, and V. Torres-Company, "Electro-optic dual-comb interferometer for high-speed vibrometry," Optics Express **25**, 16427–16436 (2017).
26. J. E. Posada-Roman, J. A. Garcia-Souto, D. A. Poiana, and P. Acedo, "Fast interrogation of fiber Bragg gratings with electro-optical dual optical frequency combs," Sensors **16**, 2007 (2016).
27. X. Yan, X. Zou, W. Pan, L. Yan, and J. Azaña, "Fully digital programmable optical frequency comb generation and application," Opt. Lett. **43**, 283–286 (2018).